

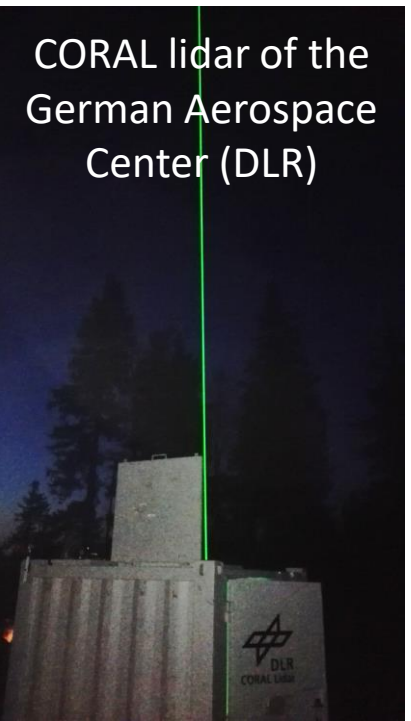
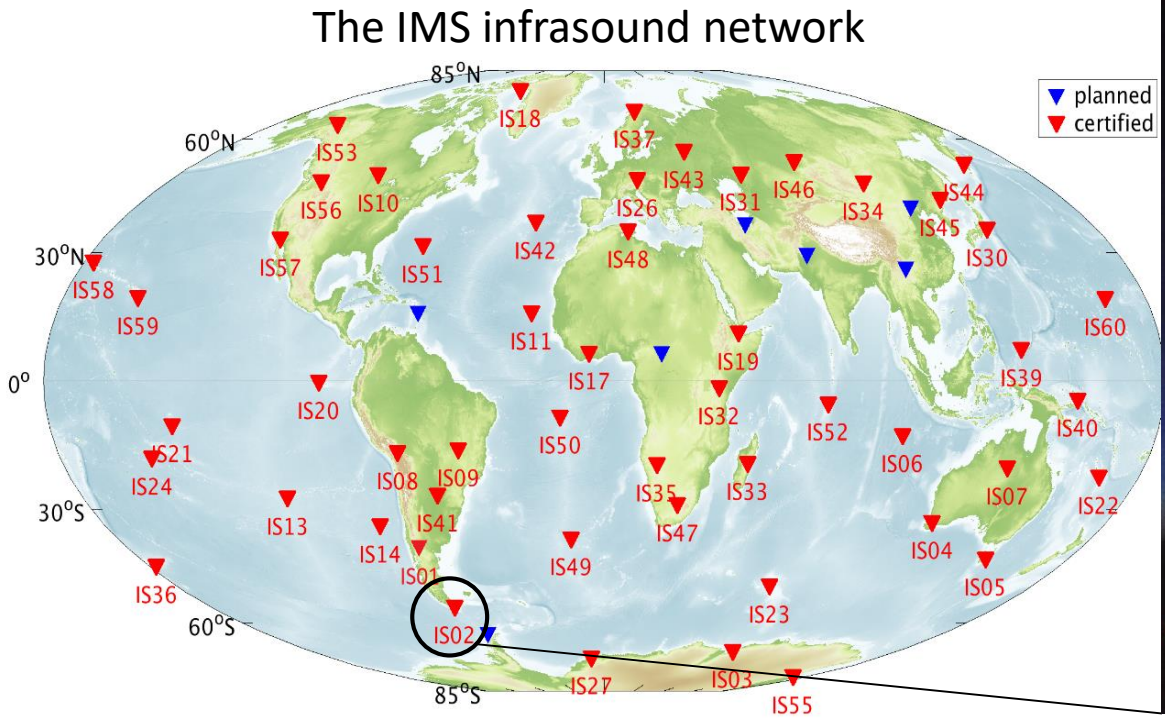
# Modelling infrasonic ocean ambient noise using NWP and lidar observations in southern Argentina

Lars Ceranna<sup>1</sup>, [Patrick Hupe](#)<sup>1</sup>,  
Marine de Carlo<sup>2</sup>, Alexis Le Pichon<sup>2</sup>

<sup>1</sup> BGR, B4.3, 30655 Hannover, Germany

<sup>2</sup> CEA, DAM, DIF, 91297 Arpajon, France

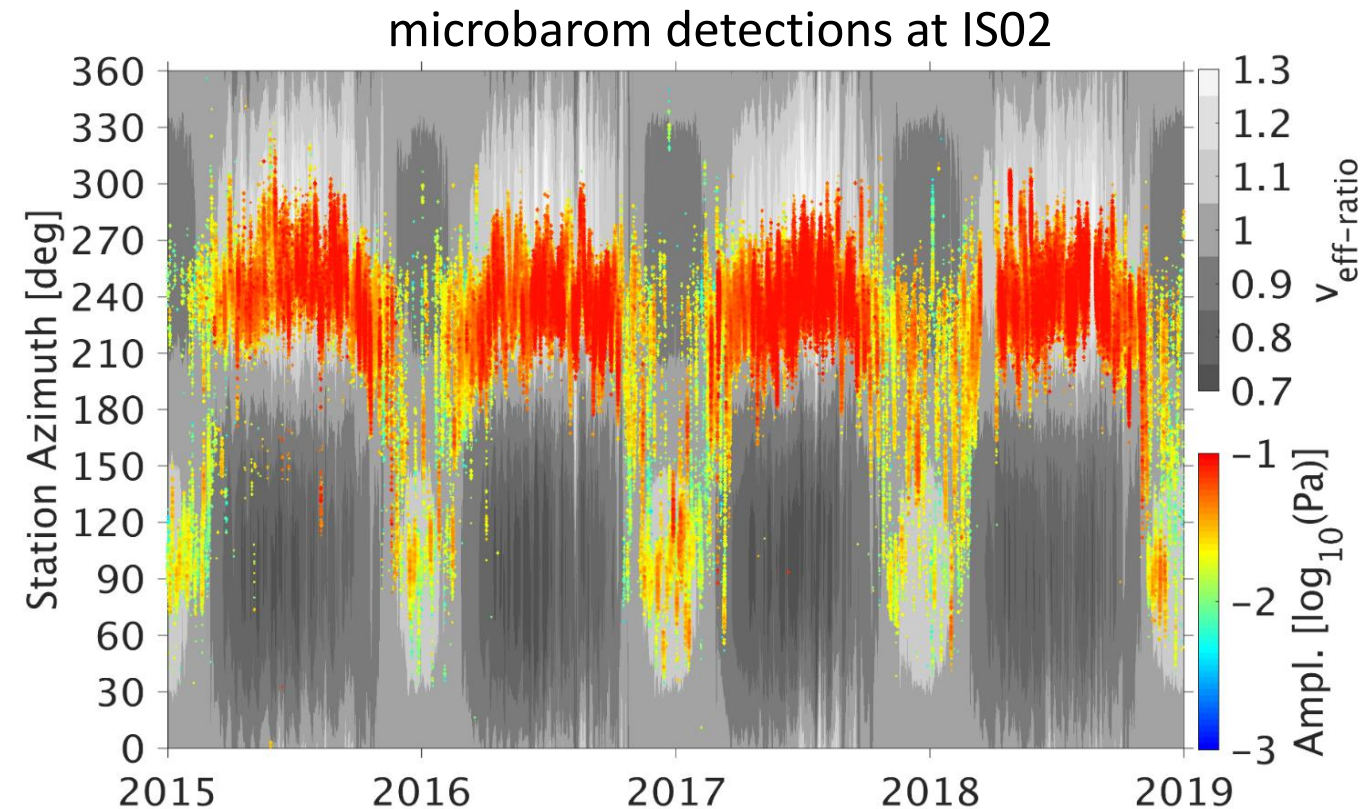
EGU2020: Sharing Geoscience Online  
Session AS1.21, Contribution D2785  
08 May 2020



CORAL lidar: deployed at about 60 km from IS02 (Kaifler et al., 2019)

## Objective: enhance the understanding of outlier detections by modelling microbaroms

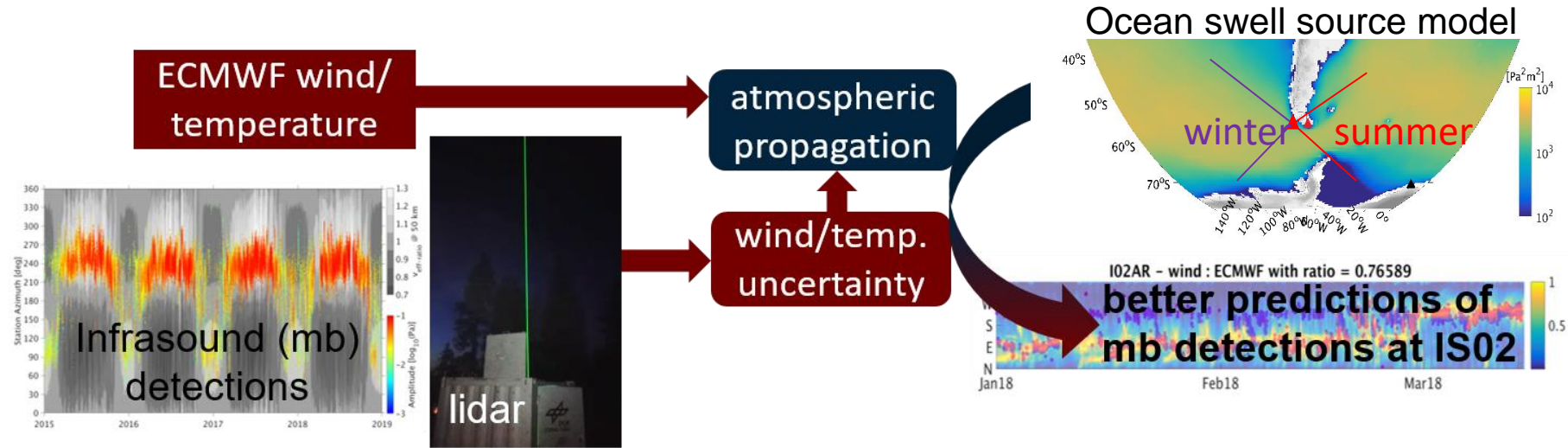
- ocean ambient noise, **microbaroms** (0.1–0.5 Hz), appear in overlapping frequency bands in the routine IMS infrasound data processing
- the seasonal variation of the middle atmosphere dynamics explains the majority of microbarom detections well, but:
- short-time fluctuations in temperature and winds lead to outlier detections



The effective sound speed ratio depicts the maximum sound speed between 40 and 60 km relative to the sound speed at the ground ( $v_{\text{eff-ratio}} \geq 1$ : favorable propagation/detection conditions). The infrasound signals were detected using the Progressive Multi-Channel Correlation (PMCC, V5.7.4) method (*Cansi, 1995*).

# A multi-technology approach for assessing numerical weather prediction (NWP) models

The principle of combining an NWP model, lidar observations and infrasound is described by *Hupe et al. (2019)* for a study at IS26. Here, the microbarom model developed by *De Carlo et al. (2020)* was applied to data of 2018.



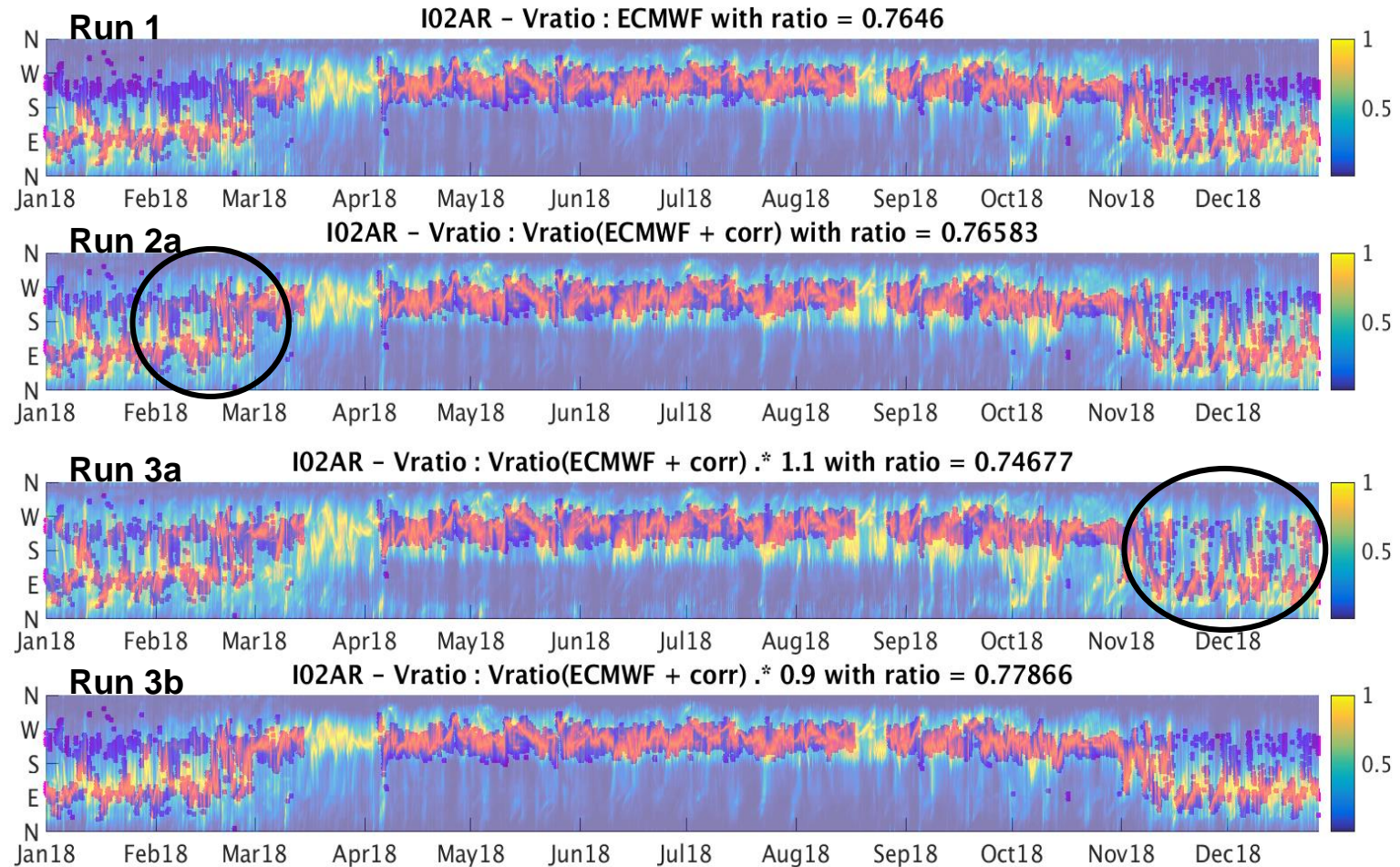
Six simulations were run, differing in the eff. sound speed ratio representing the middle atmosphere conditions:

- Standard model run: (1) ECMWF's HRES operational analysis of wind and temperature.
- Temperature-corrected runs: (2a) On a daily basis, the ECMWF temperature profiles were corrected by the mean bias as observed with DLR's temperature lidar each night (or interpolated). Temperature uncertainty – the daily  $2\sigma$  deviation was (2b) added to, and (2c) subtracted from 2a.
- Wind-corrected runs: The ECMWF effective sound speed ratio was corrected by the factors of (3a) 1.1 and (3b) 0.9, indicating strong wind perturbations that increase and decrease the effective sound speed, respectively.



## Results of the simulation runs

- very high prediction skill of the model during the winter resulting from strong sources in the west and  $v_{\text{eff-ratio}} \gg 1$
- peculiarity in the austral summer: two dominant directions of detections – not properly reflected by the ECMWF HRES analysis (Run 1)
- increased detection probability in late February and early November when adding the temperature bias (Run 2a)
- the daily  $2\sigma$  uncertainties (Runs 2b & 2c) do not result in significant changes (not shown), compared to Run 2a
- better explanation of detections from the southeast and southwest during the austral summer (Run 3a) by fictive wind perturbations (Runs 3a and 3b)



color bars: detection probability of a microbarom signal at each time step of the model (3 h); blue squares: dominant PMCC detection per time step. If a detection coincides with a probability of at least 0.8, it appears in red.

## Conclusions & Outlook

- the microbarom detections at IS02 are well explained & predicted in the winter when using the ECMWF analysis, due to the strong stratospheric duct
  - incorporating the lidar temperature observations improves the model ability to predict microbarom detections correctly in the early and late summer
  - fictive wind simulation runs show further enhancements of the microbarom prediction skill in the summer
- ➔ wind lidar observations are needed to predict microbarom detections better (especially in the summer)
- ➔ multi-directional source detection algorithm required (two dominant sources in the summer)

---

## References:

- Cansi, Y. (1995) An automatic seismic event processing for detection and location: The P.M.C.C. Method, *Geophys. Res. Lett.*, 22(9), 1021–1024, DOI:[10.1029/95GL00468](https://doi.org/10.1029/95GL00468)
- De Carlo, M., Ardhuin, F., Le Pichon, A. (2020) Atmospheric infrasound generation by ocean waves in finite depth: unified theory and application to radiation patterns, *Geophys. J. Int.*, 221(1), 569–585, DOI:[10.1093/gji/ggaa015](https://doi.org/10.1093/gji/ggaa015)
- Hupe, P., Ceranna, L., Pilger, C., De Carlo, M., Le Pichon, A., Kaifler, B., Rapp, M. (2019) Assessing middle atmosphere weather models using infrasound detections from microbaroms, *Geophys. J. Int.*, 216(3), 1761–1767, DOI:[10.1093/gji/ggy520](https://doi.org/10.1093/gji/ggy520)
- Kaifler, N., Kaifler, B., Hupe, P., Rapp, M. (2019) CORAL – An autonomous middle atmosphere lidar in southern Argentina, [Poster T1.1-P10](#) in: *Science & Technology Conference*, CTBTO, June 2019, Vienna, Austria.